

The University of Maine

DigitalCommons@UMaine

Honors College

Spring 5-2020

Using Cellulose Nanofibrils and Calcium Carbonate in Single-Use Utensils

Sierra Yost

Follow this and additional works at: <https://digitalcommons.library.umaine.edu/honors>



Part of the [Chemical Engineering Commons](#), and the [Sustainability Commons](#)

This Honors Thesis is brought to you for free and open access by DigitalCommons@UMaine. It has been accepted for inclusion in Honors College by an authorized administrator of DigitalCommons@UMaine. For more information, please contact um.library.technical.services@maine.edu.

USING CELLULOSE NANOFIBRILS AND CALCIUM CARBONATE IN
SINGLE-USE UTENSILS

by

Sierra F. Yost

A Thesis Submitted in Partial Fulfillment
of the Requirements for a Degree with Honors
(Chemical Engineering)

The Honors College

University of Maine

May 2020

Advisory Committee:

Douglas Bousfield, Professor of Chemical Engineering, Advisor
Mark Haggerty, Rezendes Preceptor for Civic Engagement in the Honors College
David Neivandt, Professor of Chemical and Biomedical Engineering
Mehdi Tajvidi, Associate Professor of Renewable Nanomaterials
Sara Walton, Lecturer in Chemical Engineering

ABSTRACT

As humanity becomes aware of the environmental issues that come from plastics, substitutes for single-use plastic are needed. Straws, expanded polystyrene, and grocery bags especially have been placed under scrutiny, but there is a need to replace other single use plastics such as eating utensils and cup lids. In this thesis, the properties of cellulose nanofibrils and calcium carbonate mixtures are characterized to determine the feasibility of their use as a plastic replacement. Using cellulose nanofibrils poses two challenges: 1) it shrinks when dried causing difficulty in forming an object, and 2) it is produced in a 3 weight percent solids suspension leading to a lot of water to remove. Pressing the water out before drying the mixture decreases shrinkage and saves money in heating utilities. Additionally, pressing the water out of the mixture decreases the shrinkage when the utensils are dried. A techno-economic analysis was performed and it was found that using a continuous refining system and a paper-machine based process to make the utensils was found to be comparable to the cost of making plastic utensils. This thesis analyzes the dewatering of CNF and CaCO_3 mixtures and the economics of creating utensils from them.

DEDICATION

This thesis is dedicated to all the men in my life, who never made me doubt that I would
one day be smarter than them (especially you, Dad).

ACKNOWLEDGEMENTS

I would like to take this time to thank all those who have supported me in this endeavor. Though I don't have time to name them all, I would like to thank my grandfather, Damien Pettinelli, who has called me at least once a week since I told him about my project to suggest trying some chemical that Dow used in the 60s that are now considered toxic. Your support means the world to me. I also would like to thank my friends and roommates, who helped me throughout this whole process. To my friends at Onyx who taught me how to conduct research, this is all because of you. And finally, to Dr. Bousfield, thank you for your continued support and help when this two-semester project became much longer because of my schedule. You are the reason this is all here today. Thank you.

TABLE OF CONTENTS

INTRODUCTION	1
Importance of Sustainability	1
Important Definitions.....	2
Current Plastic Alternatives	2
Single-Use Plastics.....	3
Cellulose Nanofibrils and Calcium Carbonate	4
Current Research.....	7
METHODS	9
Materials	9
Suspension Preparation.....	9
Dewatering Samples	9
Drying	11
Shrinkage	11
Rheology	12
Economics.....	12
RESULTS AND DISCUSSION	13
Dewatering.....	13
Drying	16
Shrinkage	17

Rheology	18
Economics	20
CONCLUSION	30
PATH FORWARD	31
Research	31
Economics	31
WORKS CITED	32
APPENDICES	35
APPENDIX A: Dewatering Data.....	36
APPENDIX B: Statistical Analysis of Data	39
APPENDIX C: Process Flow Diagram and Equipment Specifications.....	48
APPENDIX D: Equipment Specifications.....	50
APPENDIX E: Rheology Graphs	51
AUTHOR’S BIOGRAPHY	52

LIST OF TABLES

Table 1 Average Ultimate Tensile Strength and Tensile Modulus of Polypropylene and Polystyrene.....	3
Table 2: Energy Use, Water Use, Solid Waste, and CO2 Emission of Producing One Pound of Each Polymer	4
Table 3:Energy Needed for the Press after Each Vacuum Configuration	25
Table 4:Bare Module Cost of Each Piece of Equipment	27
Table 5:Cost of Manufacturing for Each Piece of Equipment.....	27
Table 6:Comparing Energy and Water Use of Plastics to CNF and CaCO3	29
Table A 1: Two Way ANOVA-determined p-values for the Difference in Means for Differing Times and Pressures	39
Table A 2: Tukey HSD Test of Significance for Time Component and 50% CNF ANOVA Data.....	39
Table A 3: Q-Test Following Tukey HSD Test for Time Component of the ANOVA Test of 50% CNF	40
Table A 4:Tukey HSD Test of Significance for Pressure Component and 50% CNF ANOVA Data.....	40
Table A 5:Q-Test Following Tukey HSD Test for Pressure Component of the ANOVA Test of 50% CNF	40
Table A 6: Tukey HSD and Q-Test for 100% CNF ANOVA Time Component	41
Table A 7:Tukey HSD and Q-Test for 100% CNF ANOVA Pressure Component.....	42
Table A 8:Equipment List and Description	48
Table A 9:Tank Specifications.....	50
Table A 10: Refiner Specifications.....	50

Table A 11: Heat Exchanger Specifications	50
Table A 12: Vacuum and Press Section Specifications	50
Table A 13: Dryer Section Specifications	50

LIST OF FIGURES

Figure 1:Ultimate Tensile Strength (Stress) and Thickness of Different Ratios of CNF to CaCO ₃	6
Figure 2:Tensile Modulus and Thickness of Different Ratios of CNF to CaCO ₃	6
Figure 3:Ultimate Wet Tensile Strength (Stress) and Thickness of Different Ratios of CNF to CaCO ₃	7
Figure 4:Wet Tensile Modulus and Thickness of Different Ratios of CNF to CaCO ₃	7
Figure 5:Diagram of Press Used for Dewatering.....	10
Figure 6:Average Shrink and Solids Before and After the Press vs. Pressure for 50/50 Mixture of CNF and CaCO ₃	13
Figure 7:Percent Solids Over Time for Different Pressures and 50/50 Mixture	14
Figure 8:Dewatering Rate (g/s) vs Time for Different Length Intervals and with and without Blotter Replacement for 50/50 Mixture of CNF and CaCO ₃ Pressed at 500psi .	15
Figure 9:Percent Solids vs. Time for Different Time Intervals and Blotter Replacement with a Mixture of 50% CNF and 50% CaCO ₃ pressed at 500psi.....	16
Figure 10:Average Shrinkage vs. Average Solids for 50/50 Mixture of CNF and CaCO ₃	17
Figure 11:Diameter of Solutions of 100% CNF after Pressing	18
Figure 12: Diameters of Different Mixtures at High Original Solids After Pressing	19
Figure 13:Diameters of Different Mixtures at Medium Original Solids After Pressing ...	19
Figure 14:Diameters of Different Mixtures at Low Original Solids After Pressing.....	20
Figure 15:Diagram of Pulp Molding Machine (TPMS Series: Molded Pulp Products Manufacturing Process, 2016)	22

Figure 16: Diagram of a Paper Machine.....	23
Figure 17:Percent Solids After the Vacuum Section vs. the Dwell Time for the Vacuums, for all Possible Combinations of Vacuums.....	23
Figure 18:Cost of Manufacturing for Vacuum and Press Section Combined	26
Figure A 1:Percent Solids Over Time for Different Pressures and 100% CNF Mixture	36
Figure A 2: Percent Solids Over Time for Different Pressures and 40% CNF 60% CaCO ₃ Mixture.....	36
Figure A 3:Percent Solids Over Time for Different Pressures and 60% CNF 40% CaCO ₃ Mixture.....	37
Figure A 4:Dewatering Rate (g/s) vs Time for Different Length Intervals and With and Without Blotter Replacement while Pressed at 500 psi for 100% CNF	37
Figure A 5:Percent Solids vs. Time for Different Time Intervals and Blotter Replacement with a Sample of 100% CNF pressed at 500psi.....	38
Figure A 6: Process Flow Diagram of Press and Drying Section.....	48
Figure A 7:Process Flow Diagram of Refining Section	48
Figure A 8: Diameter of 50% CNF 50% CaCO ₃ Material with Different Starting Solids After Pressing.....	51
Figure A 9:Diameter of 40% CNF 60% CaCO ₃ Material with Different Starting Solids After Pressing.....	51
Figure A 10:Diameter of 60% CNF 40% CaCO ₃ Material with Different Starting Solids After Pressing.....	51

CHAPTER I

INTRODUCTION

Importance of Sustainability

It is estimated that every year, 275 million metric tons (MT) of plastic waste is created worldwide (Jambeck et al., 2015). In 2010, 31.9 million MT of this was considered mismanaged, and 4.8-12.7 million MT was estimated to have ended up in the oceans (Jambeck et al., 2015). Between 60 and 95% of the litter in the ocean is estimated to come from plastic: around 50% of the plastic made each year is considered a single-use plastic (SUP). (Schnurr et al., 2018). Once in the ocean, plastic disintegrates into microplastics that are eaten by wildlife and enter the food chain. As predators eat their prey, the plastic continues up the food chain, including when humans eat fish. This is significant because it is estimated that 90% of the plastic in the ocean has degraded into pieces less than 10mm (Parker, 2017).

Since 2010, there have been worldwide initiatives to reduce the use of SUPs, most notably grocery bags and straws. More recently, countries have started to make an effort to reduce plastic cutlery usage as well. Taiwan has pledged to be SUP-free by 2030. In 2018 the European Union adopted the first ever European-wide strategy to reduce plastics, including SUP utensils. Costa Rica will be banning all SUPs in 2021, and cities all over the US are implementing their own bans (Schnurr et al., 2018). However, banning SUPs will not reduce the human desire for convenience. Already, there are single-use utensils available to fill that void and are considered more environmentally friendly than plastic polymers such as polystyrene and polypropylene. There are

substitutes made from polylactic acid, potato starch, and even banana leaves. The problem with most of these products is that they are more expensive than their plastic counterparts.

Important Definitions

There are many terms that accompany the phrase “environmentally-friendly.” When it comes to plastic replacement, biodegradable, compostable, and recyclable are common. According to the Environmental Protection Agency, biodegradable means “consumed by microorganisms and returned to compounds found in nature” and that degradation occurs within one year (*Plastic Recycling, Biodegradable and Compostable Plastics*, 2017). Every compostable material is considered biodegradable, but not every biodegradable material is considered compostable. A compostable material biodegrades into compost, which is a soil rich in nutrients. This process must occur within six months (*Plastic Recycling, Biodegradable and Compostable Plastics*, 2017). Recyclable refers to a material which would be thrown away otherwise, being reconfigured into a new product (*Recycling Basics*, 2017).

Current Plastic Alternatives

Currently, polylactic acid (PLA) is a front runner in plastic alternatives. By volume, it is the largest compostable bioplastic in use today (Cooper, 2013). PLA is derived from agricultural products such as corn, sugar beets, and potato starch (Byun & Kim, 2014). Lactic acid monomers are produced through fermentation, then turned into oligomers, depolymerized to dimers, then polymerized to PLA (Cooper, 2013). PLA can be degraded with bacteria and enzymes, specifically those in the *Pseudonocardaceae*

family. Additionally, a study done by Tokiwa and Calabia showed that protein materials such as silk, elastin, gelatin, and even some peptides and amino acids can stimulate enzyme production in microorganisms capable of degrading PLA (Tokiwa & Calabia, 2006). This means that by adding those substances to the compost the PLA will break down quicker. However, recent studies have shown that PLA is only compostable in industrial composters. This is because industrial composters are the only ones capable of reaching a temperature above 58°C, the glass transition temperature of PLA, and the temperature above which it degrades (Robertson, 2014). One of the most marketable characteristics of PLA is that it creates a waterproof barrier when melted. This also makes it harder for products made from PLA to be degraded if they get into the ocean, making it not as environmentally-friendly as it seems.

Single-Use Plastics

Most plastic utensils are made of either of two types of plastic: polypropylene and polystyrene. Table 1 shows mechanical properties of those two polymers (Flemming, n.d.).

Table 1 Average Ultimate Tensile Strength and Tensile Modulus of Polypropylene and Polystyrene (Flemming, n.d.)

Polymer	Ultimate Tensile Strength (MPa)	Tensile Modulus (GPa)
polypropylene	40	1.9
polystyrene	40	3

Research has been done about the environmental impact of the production of each type of plastic. Table 2 shows four different measurements of environmental impact, including the energy and water used, and the waste and CO₂ emissions created (Bernier,

2011). The manufacturing of polystyrene takes over 4 times more water than that of polypropylene, and produces just under 3 times the solid waste. Polystyrene production also uses around 2 kWh more per pound produced, and emits 0.84 more pounds of carbon dioxide.

Table 2: Energy Use, Water Use, Solid Waste, and CO₂ Emission of Producing One Pound of Each Polymer

Manufacturing 1 lb of material	Energy Used (kWh)	Water Used (gal.)	Solid Waste (lbs)	CO ₂ Emissions (lbs)
Polypropylene	9.34	5.12	0.029	1.67
Polystyrene	11.28	20.54	0.113	2.51

Cellulose Nanofibrils and Calcium Carbonate

Cellulose nanofibrils (CNF) are chains of plant fibers broken down, often using mechanical energy such as grinding. A cellulose fiber, which is the size of a human hair (average thickness of around 17-180 micrometers), is made up of many microfibrils. Microfibrils are bundles of nanofibrils. The nanofibrils are made of cellulosic chains, both amorphous and crystalline. The properties and potential applications of cellulose nanomaterials are reviewed by Moon et al. (2011) and Postek et al. (2013). Cellulose nanomaterials potentially can be used in packaging, construction, and automotive industries, among others, both as a binder and as a food-safe coating (Postek et al., 2013). A single microfibril of cellulose has an estimated modulus of elasticity of 70 GPa and a tensile strength of 700 MPa (Moon et al., 2011).

Calcium carbonate is found all over the world. The most common forms of CaCO₃ in nature are limestone, chalk, and marble. Chemically, all three forms are the same, but the way it is processed has an effect on its properties. Calcium carbonate from

marble can be ground into a powder form, which can be further sorted into grades by size. Calcium carbonate used from this method is called GCC, or ground calcium carbonate, and that is what CaCO_3 is referring to from here on in this thesis. Calcium carbonate can also be produced by sending CO_2 through calcium hydroxide and precipitating out the calcium carbonate that forms. This is called PCC (precipitated calcium carbonate) and results in a uniform and refined particle size of about 2 microns in diameter. PCC is currently used as a filler in the paper industry. Calcium carbonate is found in most industries, acting as a binder, filler, whitening pigment, and as a base, because it reacts to any acid and forms CO_2 . Additionally, it is used as a calcium supplement, antacid, and a base material for other medicines (*What is Calcium Carbonate?*, n.d.). Calcium carbonate is bought in a powdered form, and is much less expensive than CNF, making it a good option for a pigment to add to the CNF. Additionally, the calcium carbonate whitens the mixture, making the utensils more comparable to the single use plastic utensils used today.

When mixtures of CNF and calcium carbonate are dried, a plastic like material is formed. This material has the tensile and modulus strength properties needed for single use plastics and potentially could be used to form utensils, coffee lids, or other disposable items. Previous research in the Bousfield laboratory group, done by visiting scientist Tomohiro Onishi, determined the tensile strength of CNF and CaCO_3 mixtures. Figures 1 and 2 show the dry tensile properties for different ratios of CNF and CaCO_3 (labelled as Ca) made by Tomohiro Onishi.

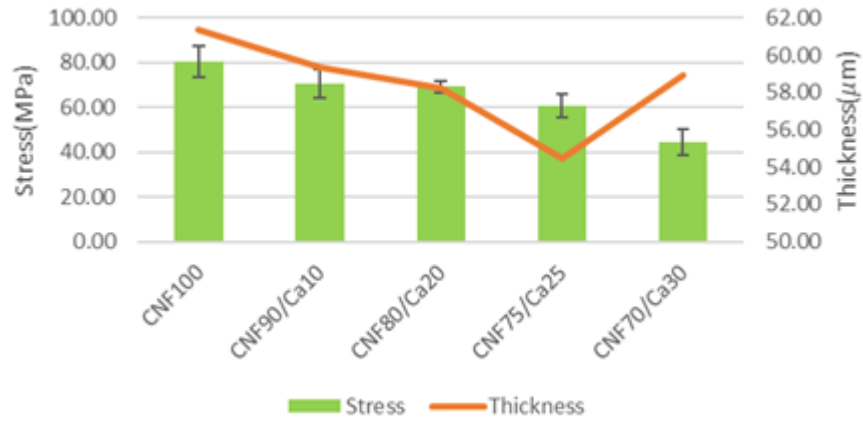


Figure 1: Ultimate Tensile Strength (Stress) and Thickness of Different Ratios of CNF to CaCO₃

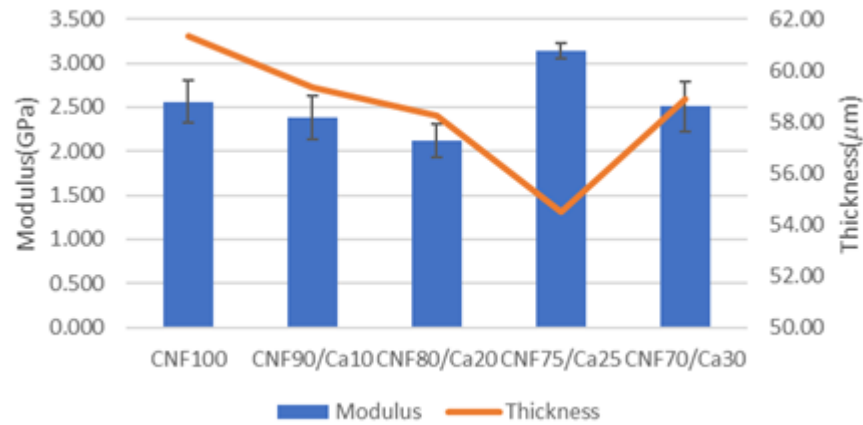


Figure 2: Tensile Modulus and Thickness of Different Ratios of CNF to CaCO₃

This data shows that the tensile strength and modulus of CNF and mixtures of CNF and CaCO₃ are comparable, or even better than plastic, as shown in Table1. For wet tensile tests, when a dried material is rewetted and tested (shown in Figures 3 and 4) on the CNF and mixtures, both values decrease, but the ultimate tensile strength is still comparable to that of polypropylene and polystyrene.

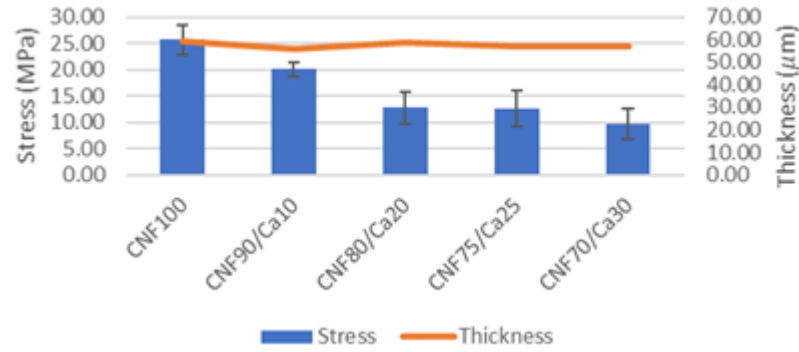


Figure 3: Ultimate Wet Tensile Strength (Stress) and Thickness of Different Ratios of CNF to CaCO_3

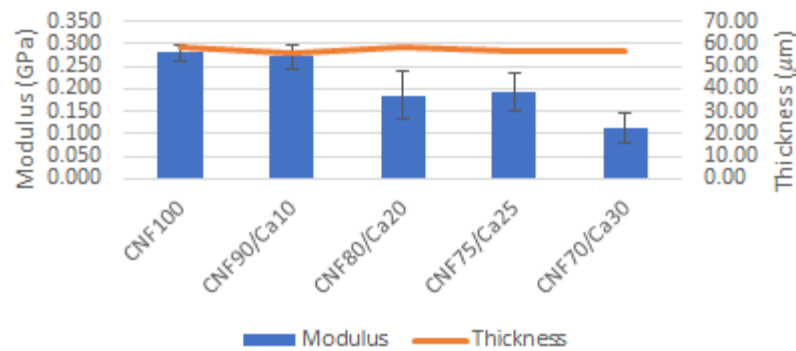


Figure 4: Wet Tensile Modulus and Thickness of Different Ratios of CNF to CaCO_3

Current Research

Much of the research done on CNF, outside of medical uses, is about its properties as a coating for packaging. CNF on paper works as a barrier for grease and oxygen; this topic has been reviewed by several recent papers such as Brodin et al. (2014) and Wang et al (2018). Two layers of CNF was found to be effective in that they cause a lower air porosity, a greater smoothness, good grease barrier and less water absorption compared to the uncoated paper; mechanical properties are improved as well (Afra et al., 2016 and Mousavi et al., 2017). Other researchers have shown that as a coating mixed with shellac resin, CNF can create a high-water barrier, as quantified for food packaging. Multiple layers of shellac and CNF adhere well to the base product, and

decrease water, air, and oxygen permeability. Other papers produced have found that as an addition to nanocomposites such as in cement-based nanocomposites, CNF makes it more lightweight, stronger, and biodegradable. The strength is from the hydrogen bonds linking the individual strands of CNF. The bonds cause the fibers to adhere to each other to create an intricate and strong web, which can enhance strength of materials mixed in it, and explains the plastic-like nature of CNF [Gardner et al., 2008]. It is also important to note that the biodegradability of cellulose was found not to change, even if broken down to the nanoscale. Additionally, studies have shown it to be non-toxic for humans and for animals, making it a low environmental hazard (Li et al., 2015). Recently, work has been done showing that the water vapor permeability of a CNF web is less than that of a normal cellulose web. Additionally, thermopressing of CNF or microwaving leads to the best final properties of a 100% CNF material, as opposed to freeze drying or using an oven. Shrinkage is minimized in those two drying methods due to compression of the material holding it in place (Rol et al., 2020).

The key idea for this thesis is to explore further the potential of CNF and calcium carbonate mixtures as a replacement for single use plastics. The dewatering properties of these mixtures were characterized as well as the drying rates. The CNF and calcium carbonate mixture was compared to plastics. Additionally, an economic analysis of making utensils at a large scale was completed.

CHAPTER II

METHODS

Materials

The materials used in this study were 3 weight percent solids cellulose nanofibrils from the University of Maine and ground calcium carbonate. The CNF is produced from bleached kraft pulp run through a refiner. The material is circulated through the refiner until the fines content is over 90% as measured with a fiber size analyzer such as MorFi or Techpap.

Suspension Preparation

CNF and calcium carbonate were weighed on an electronic balance with 0.001 precision, and hand mixed until combined for about five minutes. To get different percent mixtures of CNF and CaCO_3 , Equation 2.1 was used.

$$m_{\text{CaCO}_3} = m_{\text{CNF}} * 0.03 * \frac{x_{\text{CaCO}_3}}{x_{\text{CNF}}} \quad (2.1)$$

In this equation, the mass of CaCO_3 is calculated based on the mass of CNF used to create a ratio of x_{CNF} to x_{CaCO_3} (where x is a mass percent).

Dewatering Samples

To understand the effects of dewatering on pure CNF, 50/50 CNF and calcium carbonate mixture, a 40/60 by weight mixture, and 60/40 by weight mixture, a hand-operated hydraulic press was used. The mixtures were spread on to one half of a piece of filter paper. The filter paper was folded in half so that the mixture was completely covered, creating a semicircle. Three pieces of pulp sheets were placed on each side of

the filter paper. These were used to absorb the water that was pressed from the mixture.

Figure 5 is a diagram of this method.

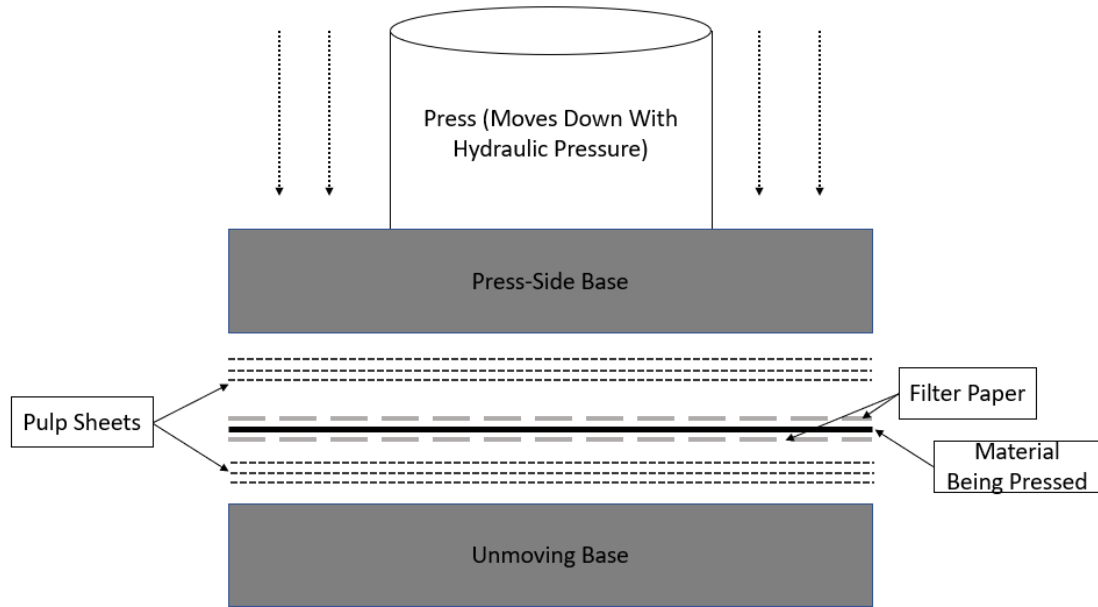


Figure 5: Diagram of Press Used for Dewatering

Initial investigation showed that no more than three blotters were needed on either side because no dampness was found on the fourth. An analog watch was used to time the amount of time the mixture was under the press. The percent solids of the mixtures after pressing and drying were determined using the Equation 2.2:

$$\%solids = \frac{m_{dry}}{m_{initial}} * 100\% \quad (2.2)$$

In Equation 2.2, $m_{initial}$ is always the mass of the mixture before pressing or drying and m_{dry} is the mass of the bone-dry final product. This does not include the weight of the filter paper the mixture is on during pressing. Dewatering rate in grams per second was calculated using Equation 2.3:

$$rate_{dewatering} = \frac{\Delta m}{\Delta t} \quad (2.3)$$

In Equation 2.3, the change in mass is in grams and the change in time is in seconds.

To get the percent solids over time and thus dewatering rate, the material being studied would be removed from the press and weighed on an electronic scale, then put back into the press. The mass of the filter paper (measured when dry) would be subtracted from the mass weighed, leaving only the mass of the material being studied and the water in it.

Drying

To dry the mixture after pressing and shaping (if done), both air drying and oven drying methods were used. Air drying was done at room temperature. For thin sheets, they were hung to dry enclosed in the filter paper, with a clothespin at the top of the semicircle holding it to a line to dry, and two clothes pins to prevent the sheet from curling. Oven drying was done on racks in a 105°C oven. For thin sheets, to prevent curling a weight was put on the sheet (still in the filter paper).

Shrinkage

To measure shrinkage of sheets, the longest length and width for each semicircle sheet was measured before and after drying. To measure the shrinkage of molded objects, 3-5 measurements were taken at different lengths and widths of the shape, then those same measurements were repeated after drying. Percent shrinkage was determined by Equation 2.4, and the average shrinkage was determined by taking the average of the percent shrinkage in multiple directions.

$$\%Shrink = \frac{d_{final} - d_{initial}}{d_{final}} * 100\% \quad (2.4)$$

Rheology

Suspensions of CNF and CaCO_3 at 100/0, 40/60, 50/50, and 60/40 were dried to different percent solids (samples are taken and dried to determine percent solids) and weighed and put into a plastic ring of a diameter of 1 in. The ring is filled until the suspension is 1 in tall and placed on a membrane then the ring is removed. Another membrane is put on top of the suspension, and 3 pieces of blotter paper were put on both sides. The layers are pressed in the hydraulic press for one minute, at 100 psi. The diameter of the solution on the membrane is measured, then it is pressed again at 500 psi for 1 minute. This is repeated for 1000, 1500, and 2000 psi.

Economics

To determine the cost of making the utensils, the following metrics were utilized: fixed capital investment (FCI), net present value (NPV), discounted cash flow rate of return (DCFROR), and cost of manufacturing (COM_d). Heuristics for the refining were used, and Aspen modelling software was used to determine the size of the dryer needed. A vacuum, press, and drying system based off of a paper machine-like setup was compared to a pulp molding-like set up to determine the most economical way to dry and form the utensils.

CHAPTER III

RESULTS AND DISCUSSION

Dewatering

Dewatering was examined for a pressure range of 0-1500 psi, with each pressure being repeated at least once, and held for one minute. It was found that as the pressure increases, higher percent solids is attainable. An ANOVA analysis proved the statistical significance of this (See Appendix 2). The opposite trend is found for the average shrinkage of each sample after oven drying. This was found while keeping the solids before the press the same at 6%.

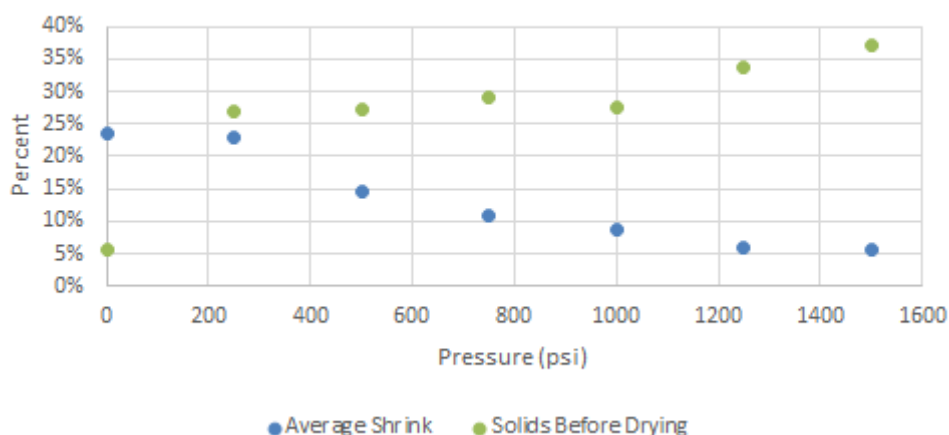


Figure 6: Average Shrink and Solids Before and After the Press vs. Pressure for 50/50 Mixture of CNF and CaCO₃

According to the Technical Association of the Pulp and Paper Industry, this is because water removal is dependent on pressure differential. The higher the pressure differential, the more water is removed (Neun, 2011). Additionally, more water removed in the press section correlates to less shrinkage when drying, so when the time of

pressing, the sample size and material, and drying stays the same as pressure increases, shrinkage decreases.

The time effect of dewatering was also analyzed. For a 50/50 mixture of CNF/CaCO₃, the amount of water removed at each press decreased over time, as seen in Figure 7.

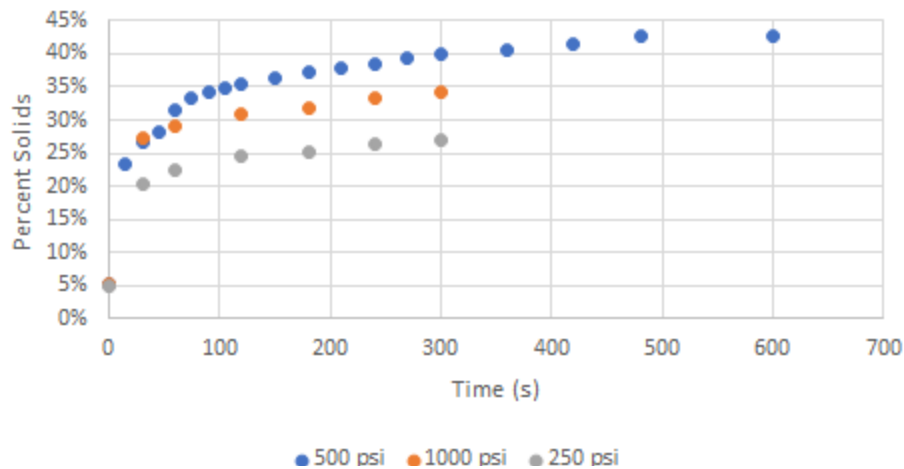


Figure 7: Percent Solids Over Time for Different Pressures and 50/50 Mixture

The percent solids in the mixture starts to plateau around 200 seconds, but the initial press removes more water than any other. This is true for all mixtures tested, as shown in Appendix 1. Dewatering rate is explicitly shown to decrease over time in Figure 8.

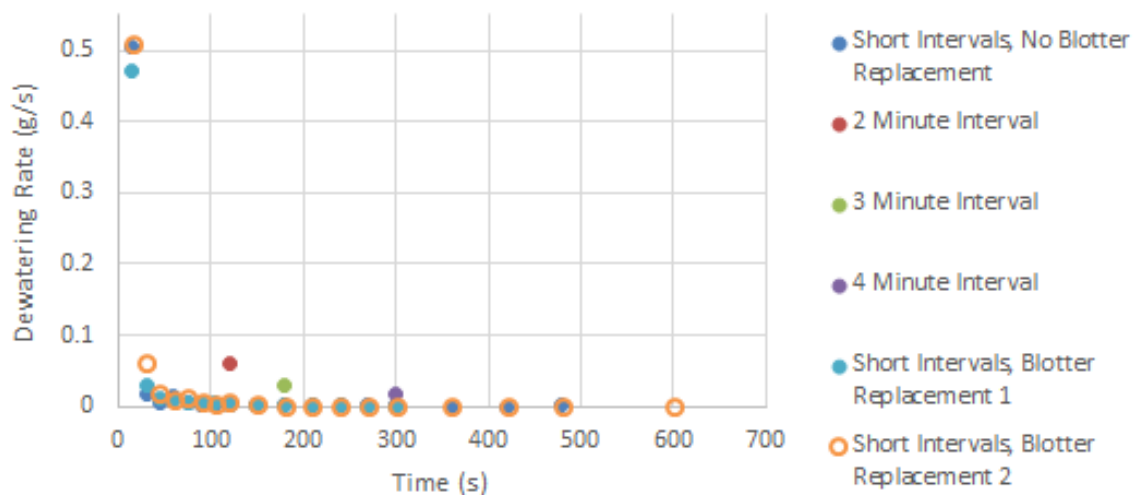


Figure 8: Dewatering Rate (g/s) vs Time for Different Length Intervals and With and Without Blotter Replacement for a 50/50 Mixture of CNF and CaCO₃ Pressed at 500psi

In Figures 8 and 9, the samples labeled 2 Minute Interval, 3 Minute Interval, and 4 Minute Interval were individual samples pressed at 500 psi for the specified amount of time without removing them to weigh them. The points labeled short intervals indicated that the sample was pressed for an interval of time, weighed to determine dewatering rate, and pressed again. The blotters on with side of the filter paper that were used to absorb the water from the sample were either replaced so they were always dry, or left the same, as indicated on the legends. It was found that more water was removed based on how many times it was pressed, not the length of time it was pressed for. That is shown in Figure 7 and Figure 8. In Figure 7 more water is removed for the 500 psi pressure than the 1000 psi pressure due to the difference in pressing frequency. Similarly, the dewatering rate over for short intervals is larger than that of one long interval, as shown in Figure 8.

The wetness outside of the sample also plays a factor in the percent solids attainable by pressing. When a 50/50 mixture of CNF and CaCO₃ was pressed multiple times and the blotters surrounding the sample were replaced so they were always dry, a

high percent solids was attained. In one trial, 90% solids were reached before the sample was put into the dryer. Another trial reached over 80%. Figure 9 shows this data. This same phenomenon appeared when the experiment was run with 100% CNF, and those results can be found in Appendix 1.

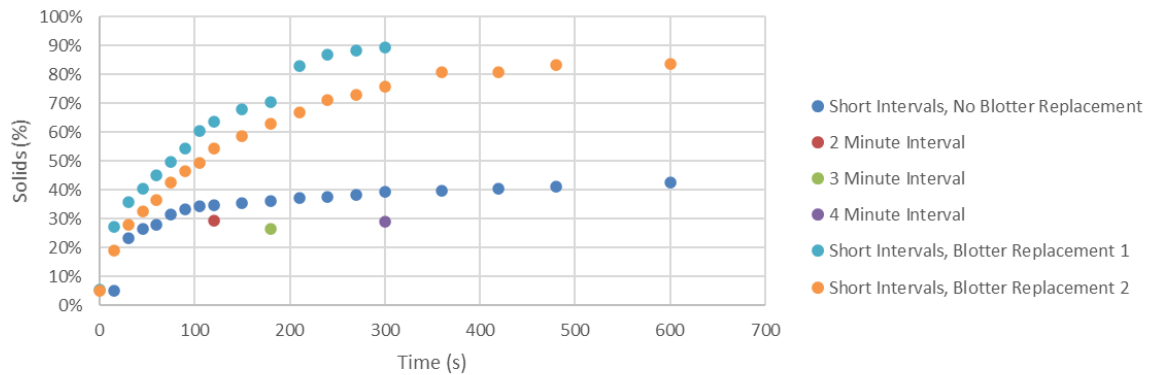


Figure 9: Percent Solids vs. Time for Different Time Intervals and Blotter Replacement with a Mixture of 50% CNF and 50% CaCO₃ pressed at 500psi

Drying

There was no change in shrinkage or final percent solids that can be attributed to different drying techniques. However, the sample curled more when air drying than oven drying, because it was hung to air dry versus being pressed in an oven. The pressing technique was the only factor that affected this quality. Drying time was the only difference in the two drying methods. In the oven the sample became bone dry in a matter of hours, where as when air drying, the sample took over 24 hours to become bone dry.

Shrinkage

As shown in Figure 6, the average shrink of the samples of 50% CNF and 50% CaCO_3 decreased as pressure used in the press increased. Figure 10 shows the relationship between the percent solids of the mixture after pressing (before drying) and the average shrink of the samples.

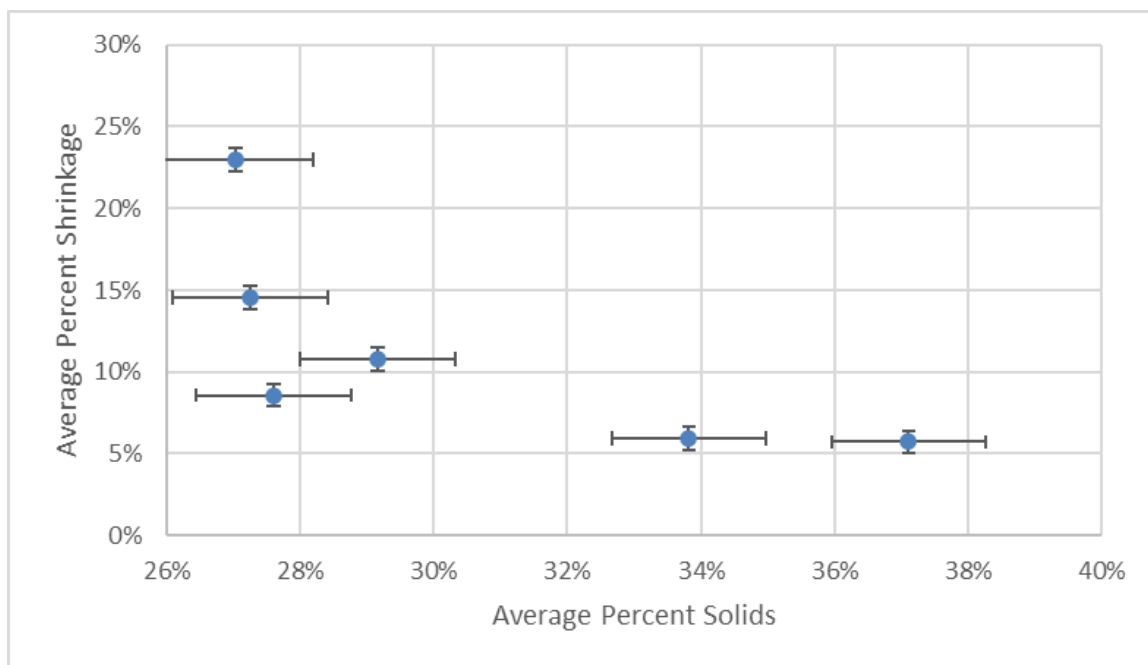


Figure 10: Average Shrinkage vs. Average Solids Entering the Oven for 50/50 Mixture of CNF and CaCO_3

A Pearson's Correlation statistical Analysis (see Appendix 2) showed that the effect of the percent solids on the average percent shrinkage is statistically significant.

Shrinkage is caused by the extensive hydrogen bonding between individual fibrils. When the fibrils are dewatered under pressure, the mechanical stress holds the fibers in place, counteracting the force of the hydrogen bonding (Gardner et al., 2008). As the percent solids of the mixture increases, the shrinkage in the oven also

decreases. This is because there is less water being removed. In the mixture of CNF, CaCO_3 , and water, the fibrils are held apart by the water. The more water that is removed, the more the CNF can collapse in on itself, causing shrinkage. By pressing water out first, CNF is in a more defined web, and therefore maintains its pressed shape more than when there is more water to be removed.

Rheology

Rheology is the study of fluid flow and deformation. Figure 11 shows the deformation of 100% CNF suspension that started at three different percent solids, and were pressed at 500, 1000, and 1500 psi.

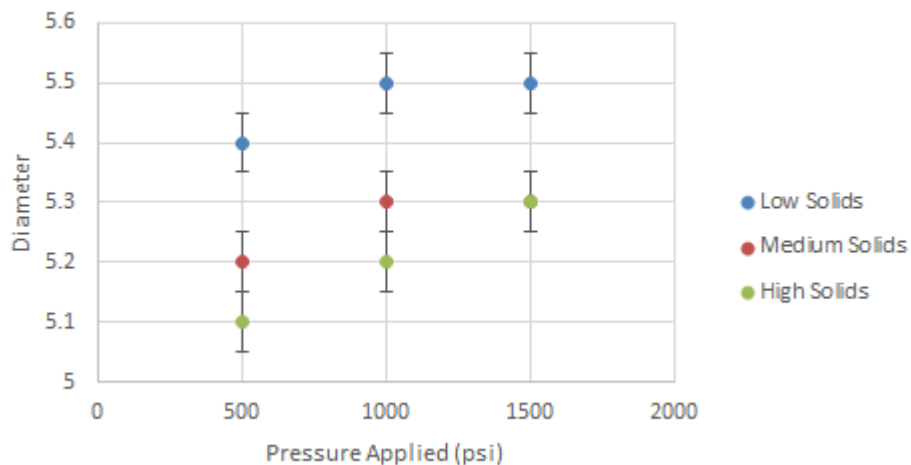


Figure 11: Diameter of Solutions of 100% CNF after Pressing

The error bars in Figure 11 show that the change in diameter between the different pressures for a single suspension are not statistically significant. The diameter is considered synonymous with the distance the suspension flows under pressure. The vertical flow of the suspension is the same for all of them, the initial height is one inch, then it is flattened, so the distance the fluid flows in horizontal direction is the factor analyzed. This experiment was repeated with 50/50, 60/40, and 40/60 mixtures of CNF

and CaCO_3 . Figures 12, 13, and 14 show the low solids, medium solids, and high solids for each of those mixtures. Appendix 5 has the graphs organized by mixture instead of solids.

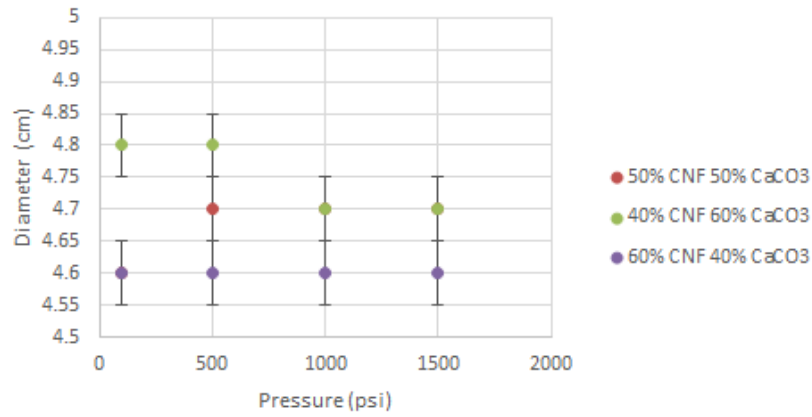


Figure 12: Diameters of Different Mixtures at High Original Solids After Pressing

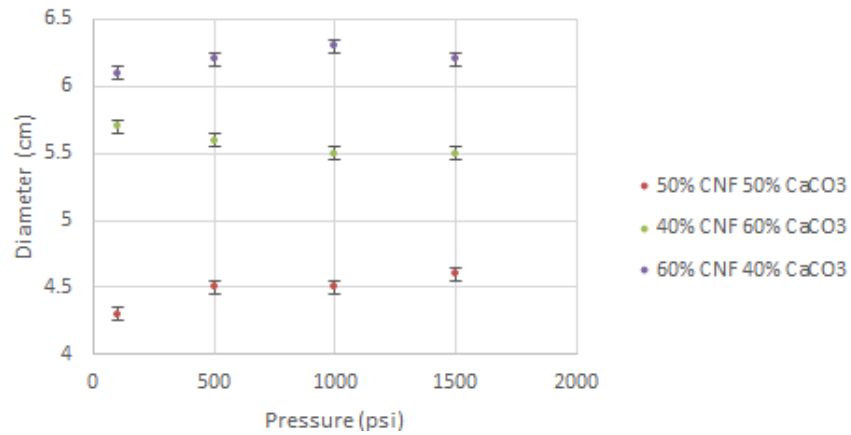


Figure 13: Diameters of Different Mixtures at Medium Original Solids After Pressing

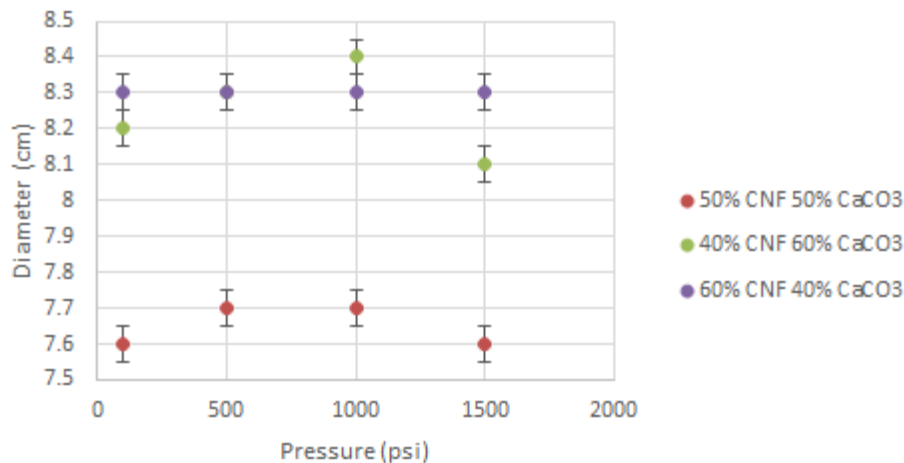


Figure 14: Diameters of Different Mixtures at Low Original Solids After Pressing

With the exception of the 40/60 mixture with a low percent starting solids (Figure 14), none of the diameters differed by a significant amount. This indicates there was no conclusive information found about the rheology of the mixtures at different starting solids. One trend to note however, is that the lower the percent solids before pressing, the more the solution deformed, and the greater the diameter became. This is due to the hydrogen bonding between the fibrils, as described in the shrinkage section.

Economics

Cellulose nanofibrils are made by refining cellulose until the nanofibrils are exposed. When designing this system, the process was assumed to be producing 200 ton/day of CNF/ CaCO₃. It was assumed the process was for a 10-year life span, a 10% internal interest rate, and a 35% tax rate. An average cost of cellulose is \$600 per ton and an average cost of the calcium carbonate is \$200 per ton. To determine profits, a sell price of \$3/lb was assumed.

First, two ways of refining of the cellulose were analyzed, a batch process and a continuous process with five consecutive refiners. The continuous refiner system was

designed with two sets of five refiners as a backup and the batch refiner also was designed with a backup. Each refiner was assumed to cost 2.5 times the cost of the drive. To create enough shear force to break the cellulose down 1.80×10^7 kJ/tonne of energy was required. The manufacturing cost (COM_d) for creating this much force for the batch system is \$77 million/ year and \$60 million / year for the continuous process. The respective fixed capital investment values (FCI) for these systems respectively are \$2.2 million and \$22.0 million (Hyde et al., 2020). Though there is a higher upfront cost associated with the continuous process, the cost saving associated with the continuous process makes it the more economic choice. A process flow diagram of this process is included in Appendix C, and refiner specifications can be found in Appendix D.

The $CaCO_3$ would then be added to refined CNF in a 4000 gallon mixing tank, which has a bare module cost of \$49,500. The mixing energy required to combine the CNF and $CaCO_3$ is 5.8 hp, which equates to a COM_d of \$6,900/ year. After the mixing tank, two options were investigated: a pulp-molding based design and a paper-machine base design. Process flow diagrams for the paper machine based model are in Appendix C. For the pulp molding machine there is only that machine after the mixing tank.

An average bare module cost for a pulp molding machine is \$650,000. In order to meet the theoretical production value of 200 tons/day, 27 of these machines must be used simultaneously. Prices for natural gas, liquid petroleum gas, and diesel oil were compared to find the most cost-effective fuel using the U.S. Energy Information Association website. Based on the prices and volumes of fuel required, natural gas was found to be the cheapest at \$147.05/day. Assuming that is the fuel used, and the maximum amount of

electricity is also used, the cost of manufacturing was calculated to be \$95,640,000/year.

Figure 15 is a diagram of a pulp-molding machine.

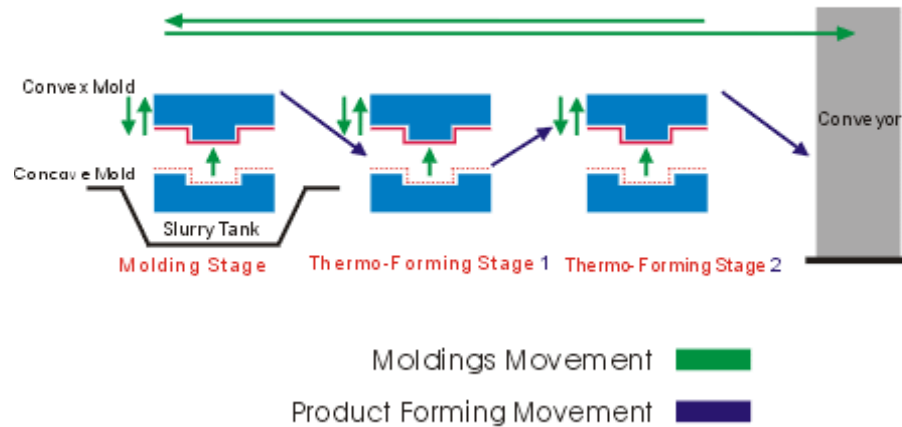


Figure 15:Diagram of Pulp Molding Machine (TPMS Series: Molded Pulp Products Manufacturing Process, 2016)

If a paper-machine based machine is used, a fourdrinier machine, vacuum section, press section, molding section, and dryer section are needed. Figure 16 shows a diagram of a paper-machine based process. To achieve a residence of time of 30 minutes in the oven, the material moves at 33 ft/min in the oven and through the fourdrinier machine. Thirty minutes is the time it takes for the remaining water to evaporate from the suspension in a 200°C oven, an average oven temperature. The conveyor belt drive for the fourdrinier machine requires 53kW of power to run at that speed. This has a bare module cost of \$108,000 and a COM_d of \$2.3 million, and the fourdrinier machine itself has a bare module cost of \$1.8 million.

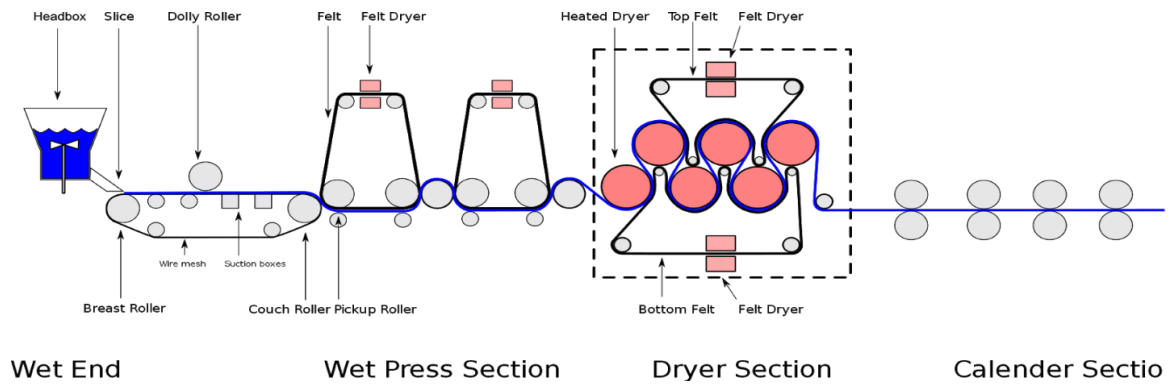


Figure 16: Diagram of a Paper Machine

The vacuum section of the machine is on the fourdrinier machine. For this system, we assumed a basis weight of 225 g/m^2 and analyzed three suction levels for vacuums: 3 in Hg, 6 in Hg, and 12 in Hg. Using these conditions, final percent solids was plotted over time for individual vacuums, and all combinations of pairs. Figure 17 shows this graph.

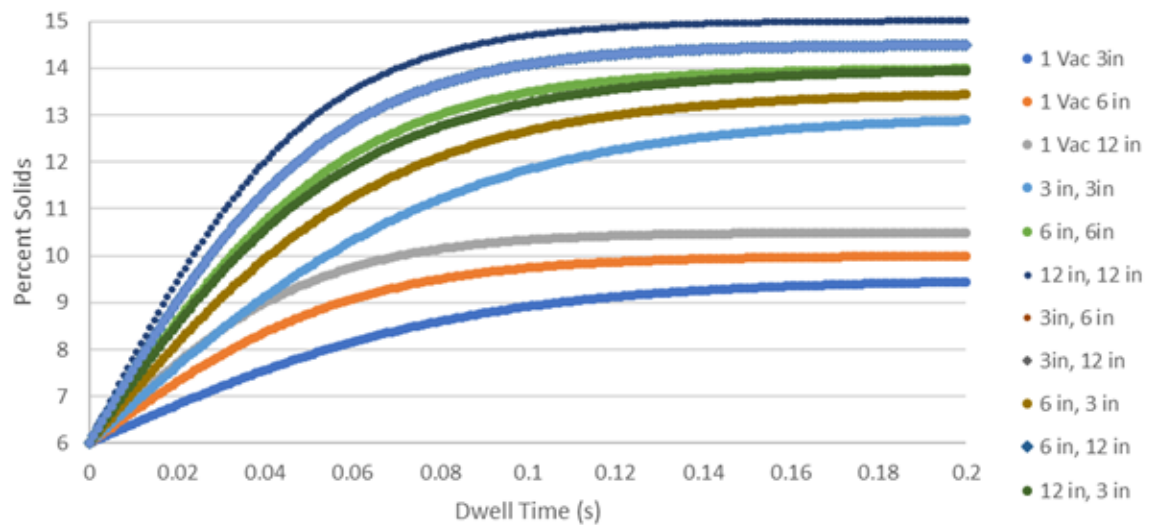


Figure 17: Percent Solids After the Vacuum Section vs. the Dwell Time for the Vacuums, for all Possible Combinations of Vacuums

From Figure 17, it was determined a dwell time of around 0.1 s was where the percent solids in the mixture started to plateau. This means that the suspension must be traveling over the vacuum for 0.1 s. It was also determined that the order of the vacuums plays no part in how much water is removed, a 12 in Hg vacuum and then a 3 in Hg vacuum in series removes the same amount of water as a 3 in Hg vacuum and 12 in Hg vacuum in series. It also shows that vacuums with more suction power remove more water.

After the vacuum is the press section. The dryer was calculated with an input of material with 50% water, so all pressing analysis was done so that the percent solids coming out of the system is 50%. That is when the molding will take place. The time required for pressing depends on the water content coming out of the vacuum section. Figure 17 shows the percent solids coming out of the vacuum section, so one vacuum with 3 in Hg suction leads to the most water entering the press section.

Table 3:Energy Needed for the Press after Each Vacuum Configuration

	t (s)	time to 50% solids	impulse pressure (kg/m*s)	line loading (N/m)	Energy (kJ)	kWh
1 Vacuum 3 in	49.1	22.1	24,400,000	512,000	476	0.132
1 Vacuum 6 in	49.1	22.1	24,400,000	512,000	476	0.132
1 Vacuum 12 in	49.1	22.1	24,400,000	512,000	476	0.132
3 in, 3 in	98.2	44.2	48,800,000	1,020,000	951	0.264
6 in, 6 in	97.3	43.8	48,300,000	1,010,000	943	0.262
12 in, 12 in	96.7	43.5	48,000,000	1,010,000	936	0.260
3 in, 6 in	97.3	43.8	48,300,000	1,010,000	943	0.262
3 in, 12 in	96.7	43.5	48,000,000	1,010,000	936	0.260
6 in, 3 in	98.2	44.2	48,800,000	1,020,000	951	0.264
6 in, 12 in	96.7	43.5	48,000,000	1,010,000	936	0.260
12 in, 3 in	98.2	44.2	48,800,000	1,020,000	951	0.264
12 in, 6 in	97.3	43.8	48,300,000	1,010,000	943	0.262

Table 3 shows that more energy is needed for the press section when there is less water removed during the vacuuming. Figure 18 shows that despite this, the cost of running one small vacuum and then pressing to 50% costs less than using vacuum suction to remove more water before the press section. Including the drive that runs the conveyor belt under the press the total equipment cost of the vacuum and press section is \$773,000 and the COM_a is \$6.806 million.

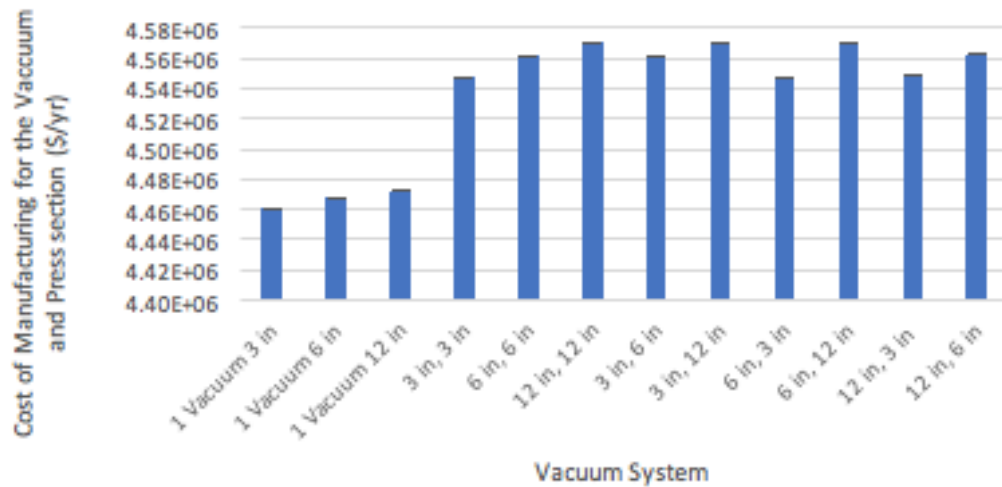


Figure 18: Cost of Manufacturing for Vacuum and Press Section Combined

Finally, the dryer section needs to remove the rest of the water, to at least 98% solids. The energy required to evaporate the water is 5,048 kW. The heat is provided by burning natural gas in a fired heater, as it is the cheapest fuel to use. To achieve that, the area of the dryer has to be 22,000 ft. It is cheapest to buy one dryer with that area as opposed to multiple dryers in series. The fire heater, dryer, and drive in the dryer cost a total bare module cost of \$5.489 million, and has a COM_d of \$2.88 million (Hyde et al., 2020). The bare module costs of the individual parts are in Table 4, and their respective COM_d values are in Table 5. Specifications about each piece of equipment can be found in the Appendix.

Table 4: Bare Module Cost of Each Piece of Equipment

Equipment	Bare Module Cost
Refiner	\$931,000
Mixing Tank	\$45,900
Fourdrinier and Drive	\$1,906,000
Press	\$25,000
Press Drive	\$106,000
Vacuum	\$642,000
Conveyor Dryer	\$2,667,000
Dryer Drive	\$325,000
Pulp Molding Machine	\$17,550,000
Gas Furnace	\$2,497,000

Table 5: Cost of Manufacturing for Each Piece of Equipment

Equipment	Cost of Manufacturing (\$/yr)
Refiner	\$86,010,000
Mixing Tank	\$7,000
Fourdrinier and Drive	\$2,335,000
Press	\$2,197,000
Press Drive	\$2,335,000
Vacuum	\$2,274,000
Conveyor Dryer	\$47,000
Dryer Drive	\$2,444,000
Pulp Molding Machine	\$10,470,000
Gas Furnace	\$397,000

Overall economic analysis was done for a 10-year life time with a 5 year MARC depreciation. With a continuous refining process and a paper-machine inspired process, the final design for the process gives a discounted cash flow rate of return (DCFROR) of 391.82%. A Monte Carlo simulation was run assuming a 5-year MARC depreciation. This analysis showed a high net present (NPV) value after ten years of \$1117.7 million, and a low NPV of \$822.1 million. The total bare module cost would be \$9,144,900 and the total COM_d would be \$108,516,000. For a pulp molding-based machine, the high NPV would be \$1098 million, and the low would be \$803.9 million according to a Monte Carlo simulation. The DCFROR would be 339.1%, making it not as profitable as the paper machine based product. Additionally, the total bare module cost would be \$21 million and the total COM_d would be \$96 million.

Comparison to Plastic

Once dry, the CNF and CaCO₃ mixture is hard and smooth, and resembles a plastic. As the previous research has shown, the strength of the mixture is comparable to plastics. A qualitative analysis of the material was done, and it was found to feel like a plastic. From a quantitative standpoint, the amount of water and energy used, and waste and CO₂ produced was also found and compared to plastic (see Table 6). The plastic comparisons were found from Dr. Andrew Bernier's paper "Living the Life of a Plastic Fork" (Bernier, 2011).

Table 6: Comparing Energy and Water Use of Plastics to CNF and CaCO₃

Manufacturing 1 lb of material	Energy Used (kWh)	Water Used (gal)	CO ₂ Emissions (lbs)
CNF and CaCO ₃	2.604	0.127	0.157
Polypropylene	9.34	5.12	1.67
Polystyrene	11.28	20.54	2.51

The energy used for CNF and CaCO₃ were calculated based on the energy requirements used for the economics section and the CO₂ emitted was based on the amount of natural gas burned in the fired heater. For every mole of natural gas burned, a mole of CO₂ is produced. The value for water used is based on the amount of water that is added to the dry cellulose pulp to create a 3% solids solution when the cellulose is being refined. This shows that not only would a CNF and CaCO₃ based utensil be less harmful for the environment after use, the production of the utensils would also have a smaller economic impact.

CHAPTER IV

CONCLUSION

This work has shown that higher pressure removes more water from the material than a lower pressure over the same amount of time. Additionally, more water can be removed if the blotters on either side of the material are dry, therefore having an increased capacity to absorb water. The more times the water is pressed, the more water is removed as well, even if it is at the same pressure over the same amount of time. More water removed in the pressing section correlates to less shrinkage in the drying section, regardless of whether the material is being air dried or oven dried.

From a process design standpoint, it was found that the paper machine process with a continuous refining system, one 3 inHg vacuum, and a dryer heated from natural gas is the most economical way to run this system. The fixed capital investment of this process is \$9 million. The rate of return and net present value are 786% and \$1.412 billion, respectively.

CHAPTER V

PATH FORWARD

Research

Future research should include the recyclability of the CNF/ CaCO₃ products. The biodegradability of CNF has been studied as has the degradability of the combination, but whether it can be added to a paper recycle stream is yet to be determined. Additionally, a feasibility study of making forks of the 50/50 solution, given the small size of the prongs is recommended. The thinness of the prongs will make them harder to mold correctly, and easier to break accidentally. A more in-depth rheology analysis on the 50/50 mixture of CNF/CaCO₃ can also be pursued to determine other uses of CNF. A molding unit needs to be designed for making the utensils before the drying section as well. A cookie-cutter type of molding system on a conveyor belt is recommended to be considered first. This would come after the press section but before the drying section.

Economics

Feasibility of creating the utensils must be further tested. In theory, the paper machine-based process will be profitable, but CNF does not drain the same way as normal cellulose pulp. For that reason, and because the molding machine was not included in the economic analysis of the system, the economic findings in this thesis are not solid conclusions and need to be further researched.

WORKS CITED

- Afra, E., Mohammadnejad, S., & Saraeyan, A. (2016). Cellulose nanofibils as coating material and its effects on paper properties. *Progress in Organic Coatings*, 101, 455–460. <https://doi.org/10.1016/j.porgcoat.2016.09.018>
- Bernier, A. (2011). *Living the Life of a Plastic Fork*. Sustainability. <https://sites.google.com/a/pvlearners.net/sustainability/a-life-cycle-analysis-a-plastic-fork>
- Brodin, F. W., Gregersen, Ø. W., & Syverud, K. (2014). Cellulose nanofibrils: Challenges and possibilities as a paper additive or coating material—A review. *Nordic Pulp & Paper Research Journal*, 29(1), 156–166.
- Byun, Y., & Kim, Y. T. (2014). Bioplastics for Food Packaging: Chemistry and Physics. In J. H. Han (Ed.), *Innovations in Food Packaging (Second Edition)* (Vol. 2, pp. 353–368). Academic Press. <https://doi.org/10.1016/B978-0-12-394601-0.00014-X>
- Cooper, T. A. (2013). Developments in bioplastic materials for packaging food, beverages and other fast-moving consumer goods. In N. Farmer (Ed.), *Trends in Packaging of Food, Beverages and Other Fast-Moving Consumer Goods (FMCG)* (pp. 108–152). Woodhead Publishing. <https://doi.org/10.1533/9780857098979.108>
- Flemming, L. (n.d.). *Tensile Property Testing of Plastics*. MatWeb. Retrieved March 9, 2020, from <http://www.matweb.com/reference/tensilestrength.aspx>
- Frequently Asked Questions about Plastic Recycling and Composting | Trash-Free Waters | US EPA*. (2017, January 19). United States Environmental Protection Agency. <https://www.epa.gov/trash-free-waters/frequently-asked-questions-about-plastic-recycling-and-composting>
- Gardner, D. J., Oporto, G. S., Mills, R., & Samir, M. A. S. A. (2008). Adhesion and Surface Issues in Cellulose and Nanocellulose. *Journal of Adhesion Science and Technology*, 22(5–6), 544–567. <https://doi.org/10.1163/156856108X295509>
- Hyde, P., Wyman, S., & Yost, S. (2020). Cellulose Nanofibrils as Single-Use Plastic Replacement [Capstone Final Report]. University of Maine.
- Jambeck, J. R., Geyer, R., Wilcox, C., Siegler, T. R., Perryman, M., Andrady, A., Narayan, R., & Law, K. L. (2015, February 13). *Plastic waste inputs from land into the ocean | Science*. Science. <https://science-sciencemag-org.wv-o-ursus-proxy02.ursus.maine.edu/content/347/6223/768.full>

- Li, F., Mascheroni, E., & Piergiovanni, L. (2015). The Potential of NanoCellulose in the Packaging Field: A Review. *Packaging Technology & Science*, 28(6), 475–508. <https://doi.org/10.1002/pts.2121>
- Moon, R. J., Martini, A., Nairn, J., Simonsen, J., & Youngblood, J. (2011). Cellulose nanomaterials review: Structure, properties and nanocomposites. *Chemical Society Reviews*, 40(7), 3941–3994.
- Neun, J. (2011, May 4). Nip Dewatering: A Press Fabric Perspective. Paper Con 2011, Covington, KY
<https://www.tappi.org/content/events/11papercon/documents/670.585%20pptx.pdf>
- Parker, L. (2017, August 16). *Ocean Life Eats Tons of Plastic—Here's Why That Matters*. National Geographic News.
<https://www.nationalgeographic.com/news/2017/08/ocean-life-eats-plastic-larvaceans-anchovy-environment/>
- Postek, M. T., Moon, R. J., Rudie, A. W., & Bilodeau, M. A. (2013). Production and applications of cellulose. *Tappi Press*.
- Recycling Basics*. (2017, January 19). United States Environmental Protection Agency.
<https://www.epa.gov/recycle/recycling-basics>
- Robertson, G. L. (2014). Food Packaging. In N. K. Van Alfen (Ed.), *Encyclopedia of Agriculture and Food Systems* (pp. 232–249). Academic Press.
<https://doi.org/10.1016/B978-0-444-52512-3.00063-2>
- Rol, F., Billot, M., Bolloli, M., Beneventi, D., & Bras, J. (2020). Production of 100% CNF object using the molded cellulose process: A feasibility study. *Industrial & Engineering Chemistry Research*.
- Schnurr, R. E. J., Alboiu, V., Chaudhary, M., Corbett, R. A., Quanz, M. E., Sankar, K., Srain, H. S., Thavarajah, V., Xanthos, D., & Walker, T. R. (2018). Reducing marine pollution from single-use plastics (SUPs): A review. *Marine Pollution Bulletin*, 137, 157–171. <https://doi.org/10.1016/j.marpolbul.2018.10.001>
- TPMS Series: Molded Pulp Products Manufacturing Process. (2016). <http://www.pulp-machinery.com/tpm%20machinery.html>
- Tokiwa, Y., & Calabia, B. P. (2006). Biodegradability and biodegradation of poly(lactide). *Applied Microbiology and Biotechnology*, 72(2), 244–251.
<https://doi.org/10.1007/s00253-006-0488-1>

Wang, J., Gardner, D. J., Stark, N. M., Bousfield, D. W., Tajvidi, M., & Cai, Z. (2018). Moisture and oxygen barrier properties of cellulose nanomaterial-based films. *ACS Sustainable Chemistry & Engineering*, 6(1), 49–70.

What is Calcium Carbonate? (n.d.). Industrial Minerals Association-North America. Retrieved March 4, 2020, from https://www.ima-na.org/page/what_is_calcium_carb

APPENDICES

APPENDIX A: Dewatering Data

The following are the dewatering over time data graphs for 100% CNF, 40% CNF and 60% CaCO₃, and 60% CNF and 40% CaCO₃ respectively.

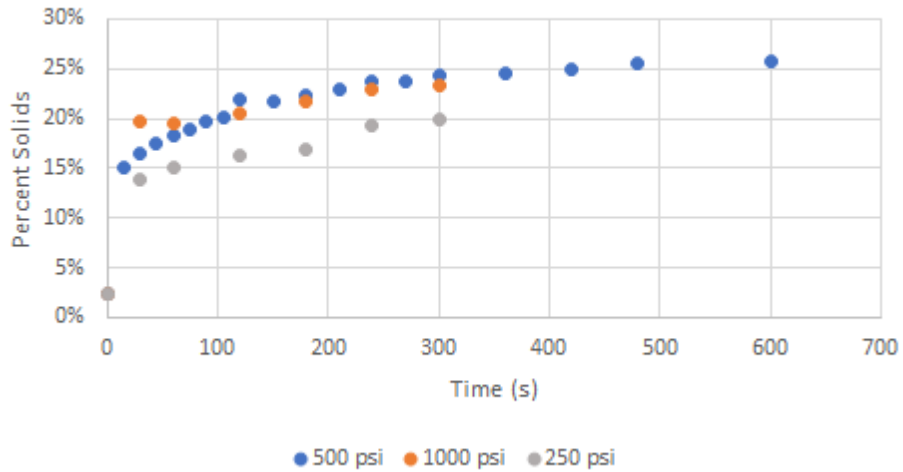


Figure A 1: Percent Solids Over Time for Different Pressures and 100% CNF Mixture

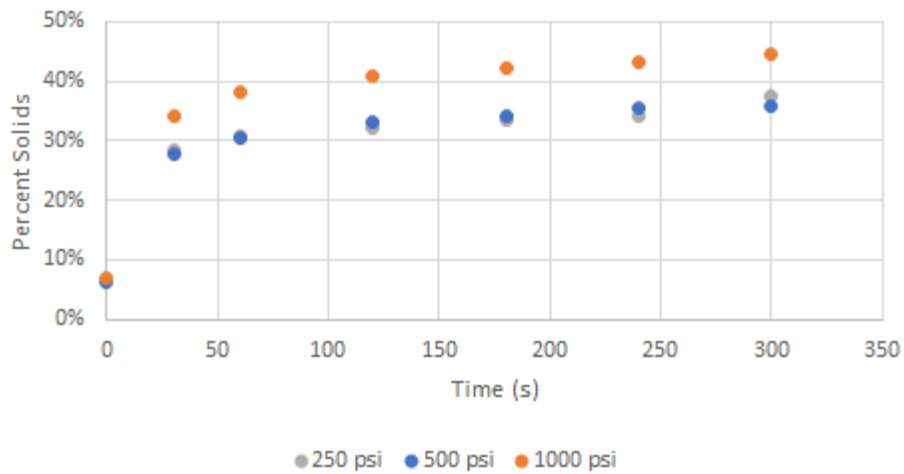


Figure A 2: Percent Solids Over Time for Different Pressures and 40% CNF 60% CaCO₃ Mixture

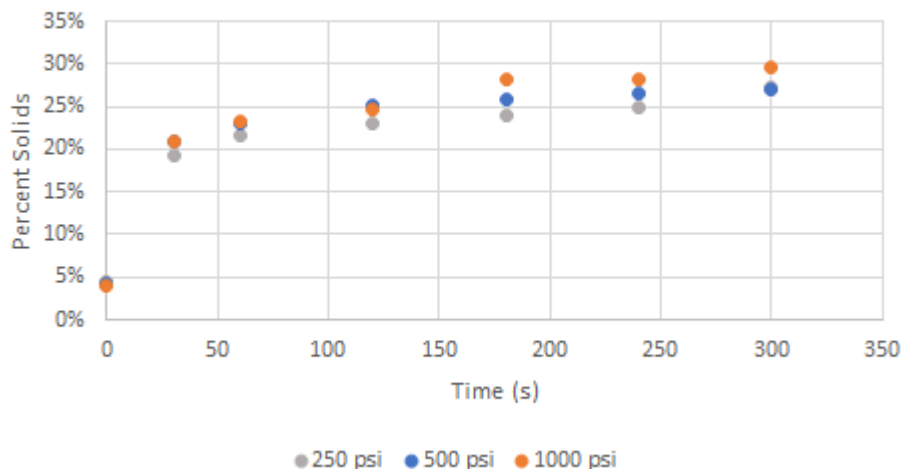


Figure A 3: Percent Solids Over Time for Different Pressures and 60% CNF 40% CaCO₃ Mixture

The following graphs show the dewatering rate data and percent solids per time data for 100% CNF when it was pressed at 500 psi for different intervals of time.

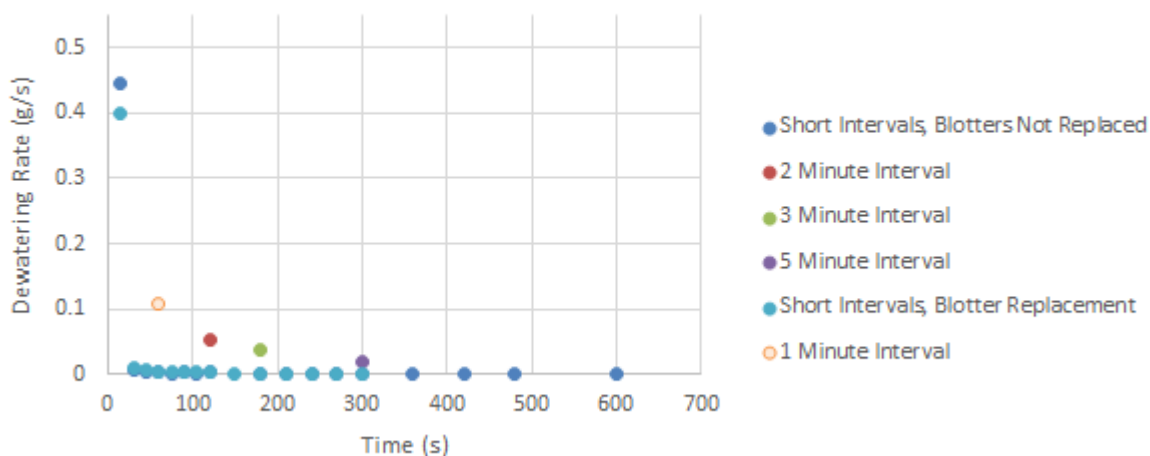


Figure A 4: Dewatering Rate (g/s) vs Time for Different Length Intervals and With and Without Blotter Replacement while Pressed at 500 psi for 100% CNF

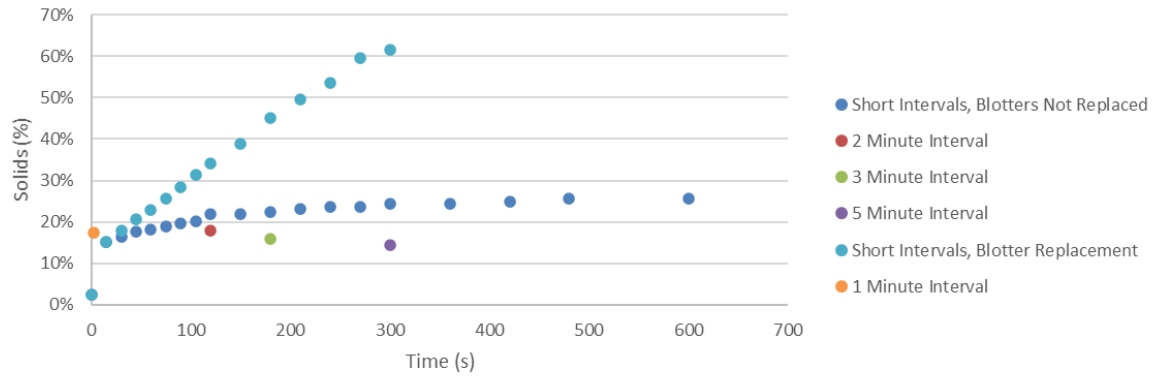


Figure A 5: Percent Solids vs. Time for Different Time Intervals and Blotter Replacement with a Sample of 100% CNF pressed at 500psi

APPENDIX B: Statistical Analysis of Data

Table A 1: Two Way ANOVA-determined p-values for the Difference in Means for Differing Times and Pressures

Concentration of CNF	p-value for pressure	p-value for time
40%	9.57E-06	3.57E-10
50%	3.73E-05	6.23E-08
60%	3.72E-03	8.39E-12
100%	1.93E-04	3.93E-09

Table A 2: Tukey HSD Test of Significance for Time Component and 50% CNF ANOVA Data

<i>group</i>	<i>mean</i>	<i>std err</i>	<i>df</i>	<i>q-crit</i>	<i>mean-crit</i>
0	0.05088				
30	0.2479				
60	0.27626				
120	0.30268				
180	0.31391				
240	0.32731				
300	0.3365				
		0.01366	12	4.95	0.06762

Table A 3: Q-Test Following Tukey HSD Test for Time Component of the ANOVA Test of 50% CNF

Q TEST						alpha	0.05
group 1	group 2	mean	q-stat	lower	upper	p-value	Cohen d
0	30	0.19703	14.4234	0.12941	0.26464	4.5E-06	8.327368257
0	60	0.22539	16.4995	0.15777	0.293	1.1E-06	9.526017319
0	120	0.2518	18.4334	0.18419	0.31942	3.1E-07	10.64254113
0	180	0.26304	19.2558	0.19542	0.33065	1.9E-07	11.11731783
0	240	0.27643	20.2363	0.20881	0.34405	1.1E-07	11.68345561
0	300	0.28563	20.9097	0.21801	0.35325	7.4E-08	12.07219704
30	60	0.02836	2.07612	-0.03926	0.09598	0.75737	1.198649062
30	120	0.05478	4.01	-0.01284	0.12239	0.14577	2.315172868
30	180	0.06601	4.83233	-0.00161	0.13363	0.05733	2.789949571
30	240	0.07941	5.81291	0.01179	0.14702	0.01811	3.356087351
30	300	0.0886	6.48623	0.02099	0.15622	0.00825	3.744828779
60	120	0.02642	1.93388	-0.0412	0.09403	0.80831	1.116523807
60	180	0.03765	2.75621	-0.02997	0.10527	0.48819	1.591300509
60	240	0.05104	3.73679	-0.01657	0.11866	0.19539	2.15743829
60	300	0.06024	4.41011	-0.00737	0.12786	0.09325	2.546179717
120	180	0.01123	0.82234	-0.05638	0.07885	0.99625	0.474776702
120	240	0.02463	1.80292	-0.04299	0.09225	0.85079	1.040914483
120	300	0.03383	2.47624	-0.03379	0.10144	0.59922	1.429655911
180	240	0.01339	0.98058	-0.05422	0.08101	0.99051	0.566137781
180	300	0.02259	1.6539	-0.04503	0.09021	0.89282	0.954879209
240	300	0.0092	0.67332	-0.05842	0.07682	0.99875	0.388741428

Note: The italicized, bold values indicate the difference between means. As the time increases, there are fewer instances of differences between means, indicating that most of the water is removed earlier in the process rather than later.

Table A 4: Tukey HSD Test of Significance for Pressure Component and 50% CNF ANOVA Data

group	mean	std err	df	q-crit	mean-crit
500 psi	0.306332073				
1000 psi	0.273878148				
250 psi	0.214976777				
		0.00894264	12	3.773	0.03374

Table A 5: Q-Test Following Tukey HSD Test for Pressure Component of the ANOVA Test of 50% CNF

Q TEST						alpha	0.05
group 1	group 2	mean	q-stat	lower	upper	p-value	Cohen d
500 psi	1000 psi	0.032453925	3.62912	-0.00129	0.06619	0.05974	1.37168
500 psi	250 psi	0.091355296	10.2157	0.05761	0.1251	2.9E-05	3.86117
1000 psi	250 psi	0.058901371	6.58657	0.02516	0.09264	0.00148	2.48949

Table A 6: Tukey HSD and Q-Test for 100% CNF ANOVA Time Component

TUKEY HSD: Two Factor Anova w/o Replications							
group	mean	std err	df	q-crit	mean-crit		
0	0.023964						
30	0.166776						
60	0.176453						
120	0.195949						
180	0.202977						
240	0.219628						
300	0.2252						
		0.007481	12	4.95	0.037029		
Q TEST						alpha	0.05
group 1	group 2	mean	q-stat	lower	upper	p-value	Cohen d
0	30	0.14281	19.09087	0.105783	0.179841	2.07E-07	11.02212
0	60	0.15249	20.38444	0.11546	0.189518	9.87E-08	11.76896
0	120	0.17198	22.99061	0.134956	0.209014	2.48E-08	13.27363
0	180	0.17901	23.9301	0.141984	0.216042	1.56E-08	13.81605
0	240	0.19566	26.15605	0.158635	0.232694	5.47E-09	15.1012
0	300	0.20124	26.90085	0.164207	0.238265	3.95E-09	15.53121
30	60	0.009677	1.293575	-0.02735	0.046706	0.962937	0.746846
30	120	0.029173	3.899742	-0.00786	0.066202	0.164297	2.251517
30	180	0.036201	4.839237	-0.00083	0.07323	0.056873	2.793935
30	240	0.05285	7.065189	0.015823	0.089881	0.004247	4.079089
30	300	0.05842	7.80998	0.021395	0.095453	0.001853	4.509094
60	120	0.019496	2.606166	-0.01753	0.056525	0.546979	1.504671
60	180	0.026524	3.545661	-0.01051	0.063553	0.237994	2.047089
60	240	0.04318	5.771614	0.006146	0.080205	0.019012	3.332243
60	300	0.04875	6.516405	0.011718	0.085776	0.007964	3.762248
120	180	0.007028	0.939495	-0.03	0.044057	0.9924	0.542418
120	240	0.02368	3.165447	-0.01335	0.060709	0.343944	1.827572
120	300	0.029251	3.910238	-0.00778	0.06628	0.162449	2.257577
180	240	0.016652	2.225952	-0.02038	0.053681	0.699789	1.285154
180	300	0.022223	2.970743	-0.01481	0.059252	0.409072	1.715159
240	300	0.005572	0.744791	-0.03146	0.042601	0.997816	0.430005

Table A 7: Tukey HSD and Q-Test for 100% CNF ANOVA Pressure Component

TUKEY HSD: Two Factor Anova w/o Replications							
<i>group</i>	<i>mean</i>	<i>std err</i>	<i>df</i>	<i>q-crit</i>	<i>mean-crit</i>		
250 psi	0.14837						
500 psi	0.18484						
1000 psi	0.18577						
		0.0049	12	3.773	0.01848		
Q TEST						alpha	0.05
<i>group 1</i>	<i>group 2</i>	<i>mean</i>	<i>q-stat</i>	<i>lower</i>	<i>upper</i>	<i>p-value</i>	<i>Cohen d</i>
250 psi	500 psi	0.03647	7.44665	0.01799	0.05495	0.00054	2.81457
250 psi	1000 psi	0.03739	7.63577	0.01892	0.05587	0.00044	2.88605
500 psi	1000 psi	0.00093	0.18913	-0.01755	0.0194	0.9902	0.07148

Table A 8: Tukey HSD and Q-Test for 40% CNF ANOVA Time Component

TUKEY HSD: Two Factor Anova w/o Replications							
<i>group</i>	<i>mean</i>	<i>std err</i>	<i>df</i>	<i>q-crit</i>	<i>mean-crit</i>		
0	0.06647						
30	0.30135						
60	0.33035						
120	0.35421						
180	0.36652						
240	0.37685						
300	0.39282						
		0.00995	12	4.95	0.04926		
Q TEST						alpha	0.05
<i>group 1</i>	<i>group 2</i>	<i>mean</i>	<i>q-stat</i>	<i>lower</i>	<i>upper</i>	<i>p-value</i>	<i>Cohen d</i>
0	30	0.23489	23.6022	0.18563	0.28415	1.8E-08	13.6267
0	60	0.26388	26.5156	0.21462	0.31315	4.7E-09	15.3088
0	120	0.28775	28.9137	0.23849	0.33701	1.7E-09	16.6933
0	180	0.30005	30.1498	0.25079	0.34931	1.1E-09	17.407
0	240	0.31038	31.1882	0.26112	0.35965	7.7E-10	18.0065
0	300	0.32636	32.7931	0.27709	0.37562	4.5E-10	18.9331
30	60	0.02899	2.91341	-0.02027	0.07826	0.42953	1.68206
30	120	0.05286	5.31154	0.0036	0.10212	0.03269	3.06662
30	180	0.06516	6.54756	0.0159	0.11442	0.00768	3.78024
30	240	0.0755	7.58599	0.02623	0.12476	0.00237	4.37977
30	300	0.09147	9.1909	0.04221	0.14073	0.00043	5.30637
60	120	0.02387	2.39813	-0.0254	0.07313	0.63083	1.38456
60	180	0.03617	3.63416	-0.0131	0.08543	0.21741	2.09818
60	240	0.0465	4.67258	-0.00276	0.09576	0.06901	2.69772
60	300	0.06247	6.27749	0.01321	0.11174	0.01051	3.62431
120	180	0.0123	1.23603	-0.03696	0.06156	0.97006	0.71362
120	240	0.02264	2.27446	-0.02663	0.0719	0.68056	1.31316
120	300	0.03861	3.87936	-0.01065	0.08787	0.16794	2.23975
180	240	0.01033	1.03843	-0.03893	0.0596	0.98727	0.59954
180	300	0.02631	2.64333	-0.02296	0.07557	0.53222	1.52613
240	300	0.01597	1.60491	-0.03329	0.06523	0.90502	0.92659

Table A 9: Tukey HSD and Q-Test for 40% CNF ANOVA Pressure Component

TUKEY HSD: Two Factor Anova w/o Replications							
<i>group</i>	<i>mean</i>	<i>std err</i>	<i>df</i>	<i>q-crit</i>	<i>mean-crit</i>		
250 psi	0.29031						
500 psi	0.29038						
1000 psi	0.35727						
		0.00652	12	3.773	0.02458		
Q TEST						alpha	0.05
<i>group 1</i>	<i>group 2</i>	<i>mean</i>	<i>q-stat</i>	<i>lower</i>	<i>upper</i>	<i>p-value</i>	<i>Cohen d</i>
250 psi	500 psi	7.2E-05	0.01108	-0.02451	0.02465	0.99997	0.00419
250 psi	1000 psi	0.06697	10.2789	0.04239	0.09155	2.7E-05	3.88506
500 psi	1000 psi	0.0669	10.2678	0.04231	0.09148	2.8E-05	3.88088

Table A 10: Tukey HSD and Q-Test for 60% CNF ANOVA Time Component

TUKEY HSD: Two Factor Anova w/o Replications							
<i>group</i>	<i>mean</i>	<i>std err</i>	<i>df</i>	<i>q-crit</i>	<i>mean-crit</i>		
0	0.04219						
30	0.20365						
60	0.22631						
120	0.24278						
180	0.25995						
240	0.26609						
300	0.2802						
		0.00523	12	4.95	0.0259		
Q TEST						alpha	0.05
<i>group 1</i>	<i>group 2</i>	<i>mean</i>	<i>q-stat</i>	<i>lower</i>	<i>upper</i>	<i>p-value</i>	<i>Cohen d</i>
0	30	0.16146	30.859	0.13556	0.18736	8.6E-10	17.8164
0	60	0.18412	35.1888	0.15822	0.21001	2E-10	20.3163
0	120	0.20059	38.338	0.17469	0.22649	7E-11	22.1344
0	180	0.21776	41.6186	0.19186	0.24366	2.1E-11	24.0285
0	240	0.22389	42.7915	0.19799	0.24979	1.4E-11	24.7057
0	300	0.23801	45.4894	0.21211	0.26391	5.1E-12	26.2633
30	60	0.02265	4.32985	-0.00324	0.04855	0.10213	2.49984
30	120	0.03913	7.47901	0.01323	0.06503	0.00267	4.31801
30	180	0.0563	10.7596	0.0304	0.0822	9.5E-05	6.21205
30	240	0.06243	11.9325	0.03653	0.08833	3.3E-05	6.88925
30	300	0.07655	14.6305	0.05065	0.10245	3.9E-06	8.4469
60	120	0.01648	3.14915	-0.00942	0.04238	0.34912	1.81816
60	180	0.03364	6.42974	0.00774	0.05954	0.0088	3.71221
60	240	0.03978	7.60268	0.01388	0.06568	0.00233	4.38941
60	300	0.05389	10.3006	0.028	0.07979	0.00015	5.94705
120	180	0.01716	3.28059	-0.00873	0.04306	0.30883	1.89405
120	240	0.0233	4.45353	-0.0026	0.0492	0.08876	2.57124
120	300	0.03742	7.15145	0.01152	0.06332	0.00385	4.12889
180	240	0.00614	1.17294	-0.01976	0.03204	0.97671	0.6772
180	300	0.02025	3.87086	-0.00565	0.04615	0.16948	2.23484
240	300	0.01412	2.69792	-0.01178	0.04002	0.51076	1.55765

Table A 11: Tukey HSD and Q-Test for 60% CNF ANOVA Pressure Component

TUKEY HSD: Two Factor Anova w/o Replications							
group	mean	std err	df	q-crit	mean-crit		
250 psi	0.20646						
500 psi	0.21825						
1000 psi	0.22722						
		0.00343	12	3.773	0.01292		
Q TEST						alpha	0.05
group 1	group 2	mean	q-stat	lower	upper	p-value	Cohen d
250 psi	500 psi	0.01179	3.44194	-0.00113	0.02471	0.07512	1.30093
250 psi	1000 psi	0.02076	6.06115	0.00784	0.03368	0.00281	2.2909
500 psi	1000 psi	0.00897	2.61921	-0.00395	0.0219	0.19495	0.98997

Table A 12: Pearson t-Test Correlation Between Shrinkage and Percent Solids After Pressing

Pearson's coeff (t test)	
Alpha	0.05
Tails	2
corr	-0.74805
std err	0.18406
t	-4.0641
p-value	0.00134
lower	-1.14569
upper	-0.3504

Table A 13: Pearson Fisher Correlation Between Shrinkage and Percent Solids After Pressing

Pearson's coeff (Fisher)	
Rho	0
Alpha	0.05
Tails	2
corr	-0.748047
std err	0.2672612
z	-3.355004
p-value	0.0007936
lower	-0.911157
upper	-0.382268

APPENDIX C: Process Flow Diagram and Equipment Specifications

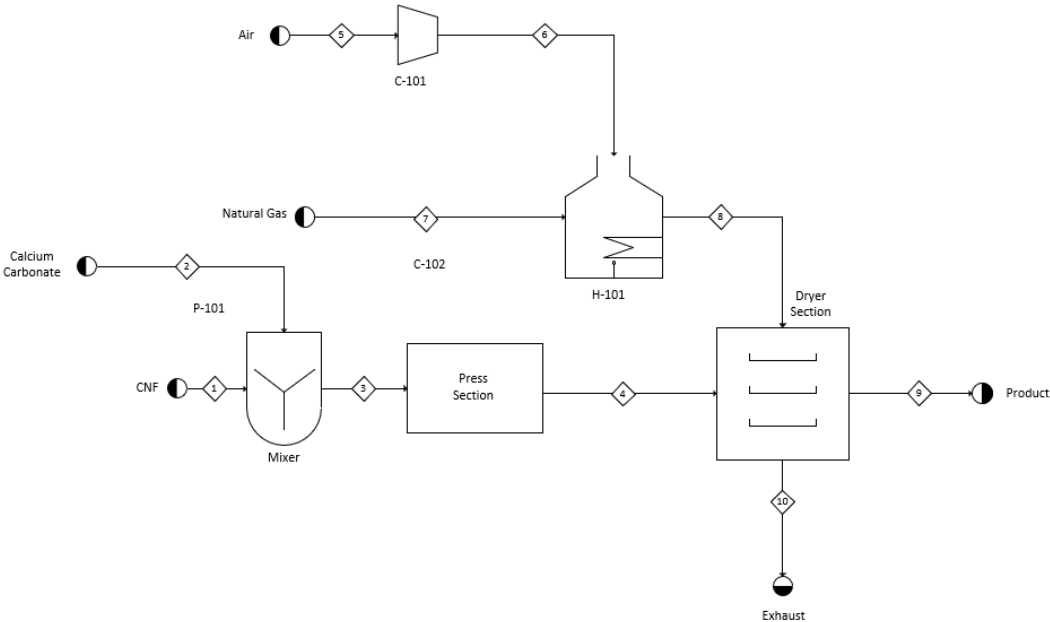


Figure A 6: Process Flow Diagram of Press and Drying Section

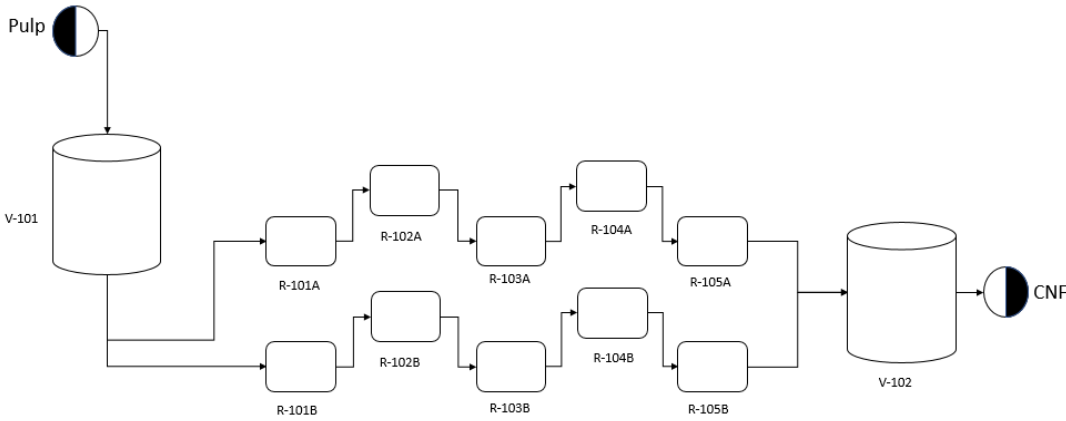


Figure A 7: Process Flow Diagram of Refining Section

Table A 14: Equipment List and Description

Unit I.D.	Description
P-101	Pump for the calcium carbonate
Mixer	Mixes the GCC with CNF
C-101	Compresses the combustion air
C-102	Compresses the natural gas
H-101	Natural gas fired heater
Press Section	Presses the CNF & GCC to 30% solids
Dryer Section	Dries the board to 95% solids
V-101	Raw pulp storage
V-102	Refined CNF storage
R-101A to R-105A	Series refiners for creating CNF
R-101B to R-105B	Series refiners for creating CNF

APPENDIX D: Equipment Specifications

Table A 15: Tank Specifications

Unit I.D.	Height (ft)	Diameter (ft)	Agitator Power Used (hp)
Mixer	14.0	6.0	5.8
V-101	16.0	10.5	1.0
V-102	16.0	10.5	2.0

Table A 16: Refiner Specifications

Unit I.D.	Type	Efficiency	Power (kW)
R-101A to R-105A	Plate refiner	0.70	1,285
R-101B to R-105B	Plate refiner	0.70	1,285

Table A 17: Heat Exchanger Specifications

Unit I.D.	Natural Gas flow rate (kg/hr)	Air mass flow rate (kg/hr)	Utility Used (kW)
H-101	388	7,048	5,048

Table A 18: Vacuum and Press Section Specifications

Unit I.D.	Description	Line Loading (kN/m)	Vacuum suction (inHg)
Press Section	One vacuum	515	3

Table A 19: Dryer Section Specifications

Unit I.D.	Area (ft ²)	Length (ft)	Width (ft)	Line Speed (ft/min)
Dryer Section	20,177	673 - 1008	20-30	22.4 - 32.6

APPENDIX E: Rheology Graphs

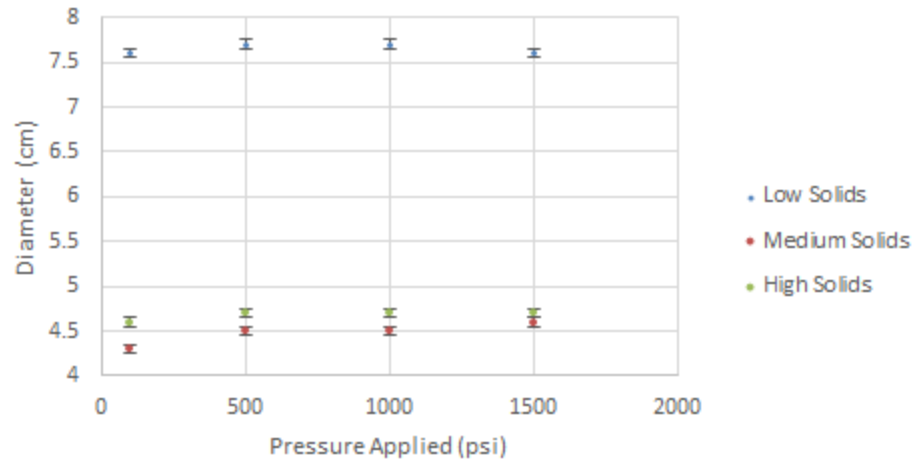


Figure A 8: Diameter of 50% CNF 50% CaCO₃ Material with Different Starting Solids After Pressing

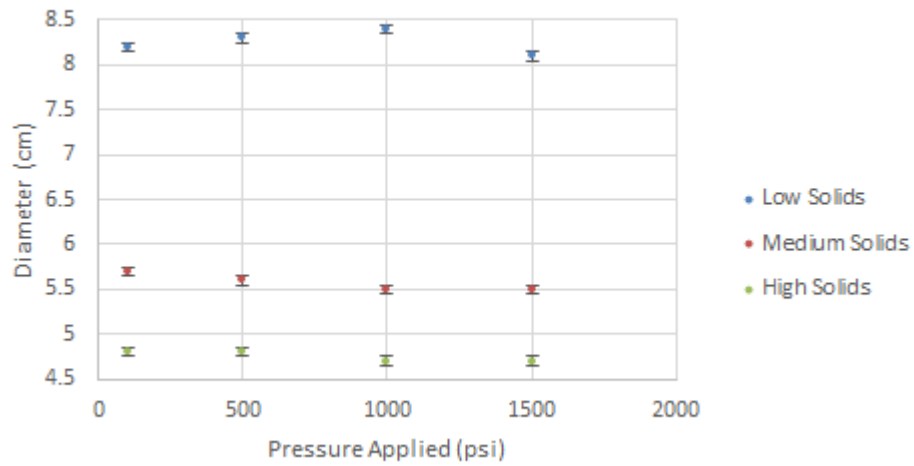


Figure A 9: Diameter of 40% CNF 60% CaCO₃ Material with Different Starting Solids After Pressing

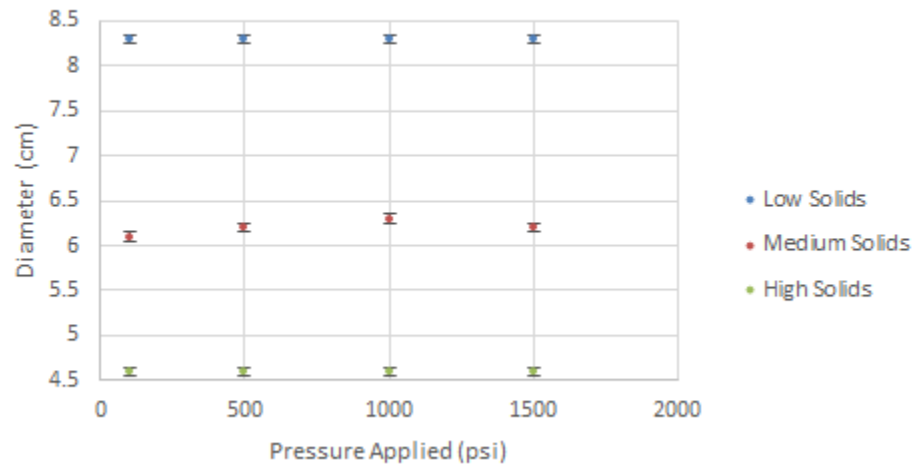


Figure A 10: Diameter of 60% CNF 40% CaCO₃ Material with Different Starting Solids After Pressing

AUTHOR'S BIOGRAPHY

Sierra Yost is a chemical engineering major in the Honors College from Windham, ME. During her time at the University of Maine, she was a part of Engineers Without Borders, American Institute of Chemical Engineers, Technical Association of the Pulp and Paper Industry, and All Maine Women. She was a Pulp and Paper Scholar and a Mitchell Scholar. She ran cross-country and track and field on the DI athletic teams and played intramural soccer with her friends. For work, she tutored her peers in math and science. At Homecoming 2019, she was part of the homecoming court. She was inducted into the Tau Beta Pi, Alpha Lambda Delta, and Phi Kappa Phi honors societies, and was chosen as the Valedictorian of the Class of 2020.

Next year, she will be attending The Pennsylvania State University to pursue her doctorate in chemical engineering, but she will always look back fondly on her time at UMaine.